Near-Optimal Detection of Zak-OTFS Signals in Doubly-Selective Channels Using Mixed Gibbs Sampling

Vineetha Yogesh and A. Chockalingam
Department of ECE, Indian Institute of Science, Bangalore 560012

***Abstract*—Recently, there has been an increasing interest in the emerging *Zak transform* based orthogonal time frequency space (OTFS), termed Zak-OTFS, owing to 1) its increased resilience to high Dopplers (compared to the multicarrier version of OTFS (MC-OTFS) that has been widely studied in the past) due to its non-fading attribute, and 2) its structured input-output relation through twisted convolution operation, which renders the input-output relation to be predictable. Zak-OTFS research is in its nascent stages and several aspects of Zak-OTFS remain open for investigation. In this paper, we investigate one such aspect, namely, signal detection in Zak-OTFS. Early papers on Zak-OTFS have considered only minimum mean square error (MMSE) detection, whose performance is far from optimum. In this work, we consider an approximate maximum a posteriori probability (MAP) detection algorithm based on mixed Gibbs sampling (MGS), where sampling is done on a mixed distribution (a weighted mixture of the target distribution and uniform distribution). The mixing with uniform distribution helps to alleviate the stalling problem witnessed in sampling purely from the target distribution. The MGS algorithm is shown to achieve better performance compared to MMSE detection as well as message passing (MP) detection, which is a widely adopted detection scheme in MC-OTFS research, and achieves near optimal performance. The closeness to optimum maximum-likelihood (ML) performance is established using a lower bound on the ML performance obtained using reactive tabu search.**

***Index Terms*—OTFS modulation, Zak-OTFS, delay-Doppler domain, mixed Gibbs sampling, approximate MAP detection.**

I. Introduction

Owing to its superior performance in high-Doppler wireless communication environments, orthogonal time frequency space (OTFS) modulation is emerging as a potential candidate for next-generation wireless [1], [2]. The superior performance is attributed to the signal processing in delay-Doppler (DD) domain as opposed to the conventional time/frequency domain processing. The channel is also parameterized in the DD domain, which facilitates a sparse representation of the channel as well as time-invariance in the DD domain over a long time. In OTFS, the information symbols are embedded in the DD domain which are subsequently converted to time domain (TD) for transmission. This conversion can be achieved in multiple ways, leading to multiple variants of OTFS. One popularly studied variant achieves this in two-steps [1], viz., the DD domain signal is first transformed to time-frequency (TF) domain using inverse symplectic finite Fourier transform and subsequently to TD using Heisenberg transform. Corresponding inverse transforms are used at the receiver to convert the received TD signal to DD domain. This variant is essentially an overlay on existing multicarrier modulation through the use of additional pre- and post-processing, hence its name multicarrier OTFS (MC-OTFS). MC-OTFS has been shown to significantly outperform OFDM in high-Doppler channels. The first wave of OTFS research was dominated by the MC-OTFS variant (e.g., references in [3]).

More recently, a single-step conversion approach based on Zak transform theory [4], named Zak-OTFS, is gaining prominence due to its strong mathematical foundation, structured input-output relation through twisted convolution operation, and augmented resilience to a larger range of Doppler spreads compared to MC-OTFS [5], [6]. The early Zak-OTFS references [5], [6] reveal the foundational aspects of Zak-OTFS, especially its 'non-fading' channel interaction and 'predictability' of the input-output relation, attributed to the better localization of the Zak-OTFS waveform in the DD domain. Zak-OTFS waveform is a quasi-periodic pulse in the DD domain, localized within the fundamental period with τ_p and ν_p being the delay and Doppler periods. Zak transform enables a direct conversion of signals from TD to DD domain and vice-versa. Upon conversion from DD domain to TD using inverse Zak transform, Zak-OTFS waveform is a pulse train modulated by a tone, referred to as a 'pulsone'.

We note that Zak-OTFS research is in its nascent stages and several aspects of Zak-OTFS remain open for investigation. In this paper, we investigate one such aspect, namely, signal detection in Zak-OTFS. In this regard, we note that the early Zak-OTFS papers [5], [6] consider only minimum mean square error (MMSE) detection, whose complexity is polynomial (cubic) in the OTFS frame size but performance is far from optimum. On the other hand, optimum maximum likelihood (ML) detection is prohibitively complex for large frame sizes of practical interest (due to exponential complexity in frame size). Therefore, detection algorithms which can achieve near-optimum performance with practical complexities are of interest for Zak-OTFS receivers.

Motivated by the above, in this paper, we explore Markov chain Monte Carlo (MCMC) techniques for Zak-OTFS signal detection. MCMC techniques are computational techniques that make use of sampling from probability distributions in order to make statistical inferences by simulating the underlying processes through Markov chains, making it possible to reduce the complexity from exponential to polynomial [7]. Gibbs sampling is a popular MCMC method. MCMC methods have been adopted for detection/equalization in MIMO channels, ISI channels, and OFDM in time-varying channels [8]- [11]. Our contributions in this paper can be summarized as follows.

This work was supported in part by the J. C. Bose National Fellowship, Department of Science and Technology, Government of India. The first author would like to thank the Prime Minister's Research Fellowship, Ministry of Education, Government of India for the support.

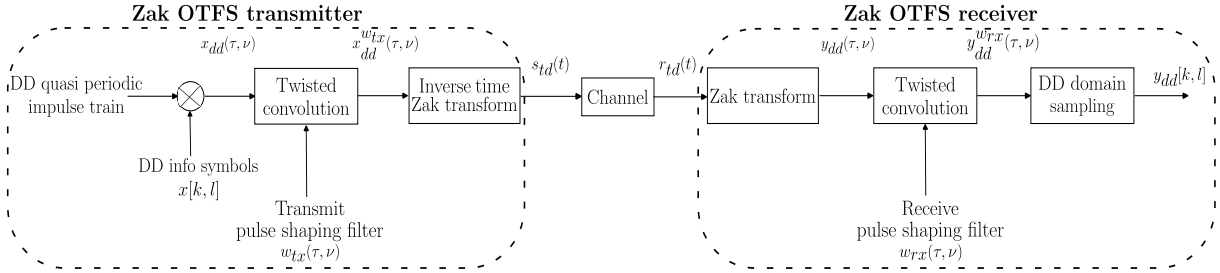

Fig. 1: Block diagram of Zak-OTFS transceiver.

- We consider an approximate maximum a posteriori probability (MAP) detection algorithm based on mixed Gibbs sampling (MGS), where sampling is done on a mixed distribution (a weighted mixture of the target distribution and uniform distribution). The mixing with uniform distribution helps to alleviate the stalling problem witnessed in sampling purely from the target distribution.
- The MGS algorithm is shown to achieve much better performance compared to MMSE detection as well as message passing (MP) detection, which is a widely used detection scheme in MC-OTFS research [13], [14].
- Using a lower bound on the ML performance obtained using reactive tabu search (RTS) [15], we demonstrate the closeness of the MGS performance to the optimum ML performance.

II. Zak-OTFS system model

Figure 1 shows the block diagram of the Zak-OTFS transceiver. At the transmitter, a continuous-time quasi-periodic DD domain signal $x_{\text{dd}}^{\text{w}_{\text{tx}}}(\tau,\nu)$ is converted to TD using inverse time-Zak transform, resulting in a TD signal $s_{\text{td}}(t)$. At the receiver, the TD signal $r_{\text{td}}(t)$ is converted to a DD domain signal $y_{\text{dd}}(\tau,\nu)$ using Zak transform which further undergoes DD domain processing.

At the transmitter, MN information symbols from a modulation alphabet $\mathbb{A}$, denoted by $x[k,l]$s, are mounted on the DD domain information grid Λ_{dd} described as

$$\Lambda_{\text{dd}} = \left\{ \left(\frac{k\tau_p}{M}, \frac{l\nu_p}{N} \right); k \in [0, M-1], l \in [0, N-1] \right\}, \quad (1)$$

where τ_p and ν_p denote the period along delay and Doppler axis of the fundamental box/rectangle $\mathcal{D}_0$, described as

$$\mathcal{D}_0 = \{(\tau,\nu); 0 < \tau < \tau_p, 0 < \nu < \nu_p\}, \quad (2)$$

such that $\tau_p \nu_p = 1$. The $x[k,l]$s are encoded as discrete DD information signal $x_{\text{dd}}[k,l]$, given by

$$x_{\text{dd}}[k+nM, l+mN] = x[k,l] e^{j2\pi n \frac{l}{N}}, \quad (3)$$

where $k = 0, 1, \cdots M-1$, $l = 0, 1, \cdots, N-1$, and $n, m \in \mathbb{Z}$. Note that $x_{\text{dd}}[k,l]$ is a quasi-periodic signal [6]. These symbols are then mounted onto a continuous-time impulse train resulting in a quasi-periodic DD domain signal $x_{\text{dd}}(\tau,\nu)$, given by

$$x_{\text{dd}}(\tau,\nu) = \sum_{k,l \in \mathbb{Z}} x_{\text{dd}}[k,l] \delta\left(\tau - k\frac{\tau_p}{M}\right) \delta\left(\nu - l\frac{\nu_p}{N}\right), \quad (4)$$

where $\delta(\cdot)$ denotes Kronecker delta function. Further, the signal is time- and band-limited by filtering it through the transmit DD filter $w_{\text{tx}}(\tau,\nu)$, resulting in

$$x_{\text{dd}}^{\text{w}_{\text{tx}}}(\tau,\nu) = w_{\text{tx}}(\tau,\nu) *_\sigma x_{\text{dd}}(\tau,\nu), \quad (5)$$

where $*_\sigma$ denotes the twisted convolution operation. Note that this DD domain pulse has a spread of approximately $\frac{1}{B}$ along delay axis and $\frac{1}{T}$ along Doppler axis, where $B \approx M\nu_p$ is the bandwidth and $T \approx N\tau_p$ is the frame duration. The resulting continuous DD domain signal $x_{\text{dd}}^{w_{\text{tx}}}(\tau,\nu)$ is converted to TD using inverse time-Zak transform, given by

$$s_{\text{td}}(t) = \mathcal{Z}_t^{-1}\left(x_{\text{dd}}^{w_{\text{tx}}}(\tau,\nu)\right) = \sqrt{\tau_p} \int_0^{\nu_p} x_{\text{dd}}^{w_{\text{tx}}}(t,\nu) d\nu. \quad (6)$$

The TD signal $s_{\text{td}}(t)$ passes through a doubly-selective channel with DD domain impulse response

$$h(\tau,\nu) = \sum_{i=1}^{P} h_i \delta(\tau - \tau_i) \delta(\nu - \nu_i), \quad (7)$$

where P is the number of resolvable paths in DD domain, h_i, τ_i, ν_i denote the channel gain, delay, and Doppler of the ith path, respectively. The resulting TD signal at the receiver is given by

$$r_{\text{td}}(t) = \int\int h(\tau,\nu) s_{\text{td}}(t-\tau) e^{j2\pi\nu(t-\tau)} + n(t), \quad (8)$$

where $n(t)$ is the additive white Gaussian noise (AWGN). The received signal is converted to DD domain using Zak transform as

$$\begin{aligned} y_{\text{dd}}(\tau,\nu) &= \mathcal{Z}_t(r_{\text{td}}(t)) \\ &= \sqrt{\tau_p} \sum_{k \in \mathbb{Z}} r_{\text{td}}(\tau + k\tau_p) e^{-j2\pi\nu k\tau_p} + n_{\text{dd}}(\tau,\nu), \end{aligned} \quad (9)$$

where $n_{\text{dd}}(\tau,\nu) = \mathcal{Z}_t(n(t))$ is the DD domain noise signal. The continuous DD domain received signal $y_{\text{dd}}(\tau,\nu)$ is then filtered using DD domain receive filter $w_{\text{rx}}(\tau,\nu)$ to obtain $y_{\text{dd}}^{w_{\text{rx}}}(\tau,\nu)$ as

$$\begin{aligned} y_{\text{dd}}^{w_{\text{rx}}}(\tau,\nu) &= w_{\text{rx}}(\tau,\nu) *_\sigma y_{\text{dd}}(\tau,\nu) \\ &= h_{\text{dd}}(\tau,\nu) *_\sigma x_{\text{dd}}(\tau,\nu) + n_{\text{dd}}^{w_{\text{rx}}}(\tau,\nu), \end{aligned} \quad (10)$$

$$x(\tau,\nu) *_\sigma y(\tau,\nu) = \int\int x(\tau',\nu') y(\tau-\tau', \nu-\nu') e^{j2\pi\nu'(\tau-\tau')} d\tau' d\nu'$$

where $h_{\text{dd}}(\tau,\nu)$ is the effective continuous DD channel filter, given by

$$h_{\text{dd}}(\tau,\nu) = w_{\text{rx}}(\tau,\nu) *_\sigma h(\tau,\nu) *_\sigma w_{\text{tx}}(\tau,\nu). \quad (11)$$

The resulting signal is sampled on the information grid Λ_{dd} to obtain the discrete DD domain received signal as

$$y_{\text{dd}}[k,l] = y_{\text{dd}}^{w_{\text{rx}}}\left(\tau = k\frac{\tau_p}{M}, \nu = l\frac{\nu_p}{N}\right), \quad k,l \in \mathbb{Z}. \quad (12)$$

The end-to-end DD domain input-output relation can be expressed as

$$y_{\text{dd}}[k,l] = h_{\text{dd}}[k,l] *_\sigma x_{\text{dd}}[k,l] + n_{\text{dd}}[k,l], \quad (13)$$

where $h_{\text{dd}}[k,l] = h_{\text{dd}}\left(\tau = k\frac{\tau_p}{M}, \nu = l\frac{\nu_p}{N}\right), k,l \in \mathbb{Z}$. Using the definition of discrete twisted convolution in (13), we obtain

$$y_{\text{dd}}[k,l] = \sum_{k',l' \in \mathbb{Z}} h_{\text{dd}}[k-k', l-l'] x_{\text{dd}}[k',l'] e^{j2\pi\frac{(l-l')k'}{MN}} + n_{\text{dd}}[k,l]. \quad (14)$$

The above expression can be vectorized as

$$\mathbf{y} = \mathbf{H}\mathbf{x} + \mathbf{n}, \quad (15)$$

where $\mathbf{y}, \mathbf{x}, \mathbf{n} \in \mathbb{C}^{MN\times 1}$, such that their $(kN+l+1)$th entries are given by $y_{kN+l+1} = y_{\text{dd}}[k,l]$, $x_{kN+l+1} = x_{\text{dd}}[k,l]$, and $n_{kN+l+1} = n_{\text{dd}}[k,l]$, and $\mathbf{H} \in \mathbb{C}^{MN\times MN}$ such that

$$\mathbf{H}[k'N+l'+1, kN+l+1] = \sum_{m,n\in\mathbb{Z}} h_{\text{dd}}[k'-k-nM, l'-l-mN] e^{j2\pi nl/N} e^{j2\pi\frac{(l'-l-mN)(k+nM)}{MN}}, \quad (16)$$

where $k', k = 0,1,\cdots,M-1, l', l = 0,1,\cdots,N-1$, and $\mathbf{n} \sim \mathcal{CN}(\mathbf{0}, \sigma^2\mathbf{I}_{MN})$, where $\mathbf{0}$ denotes a zero vector of length MN and $\mathbf{I}_{MN}$ is an identity matrix of size MN.

III. Zak-OTFS signal detection using MGS

In this section, we present the proposed approximate MAP detection algorithm based on mixed Gibbs sampling (MGS) for symbol detection in Zak-OTFS. We also present the MMSE detector and MP detector which are used for performance comparison.

A. Approximate MAP detection algorithm based on MGS

The maximum a posteriori probability (MAP) detection rule for the input-output relation in (15), assuming perfect channel knowledge, is given by

$$\hat{\mathbf{x}}_{\text{MAP}} = \arg\max_{\mathbf{x}\in\mathbb{A}^{MN}} \text{P}(\mathbf{x}|\mathbf{y},\mathbf{H}), \quad (17)$$

where $\text{P}(a|b)$ denotes the conditional probability density function (pdf) of a given b. An exhaustive enumeration of all possible MN length vectors drawn from $\mathbb{A}$ is required to solve (17), i.e., $|\mathbb{A}|^{MN}$ unique vectors. This number grows exponentially as MN increases rendering an exhaustive enumeration based solution to (17) infeasible. Hence, a reduced complexity detection algorithm based on MCMC approach using Gibbs sampling (GS) is employed. Note that for the case under consideration, ML solution and MAP solution are same since all the symbols have equal prior probability, i.e., $1/MN$. The target distribution that guarantees optimal solution is

$$\text{P}(x_1, x_2, \cdots, x_{MN}|\mathbf{y},\mathbf{H}) \propto \exp\left(\frac{||\mathbf{y}-\mathbf{H}\mathbf{x}||^2}{\sigma^2}\right). \quad (18)$$

However, directly sampling from this joint distribution is complex. Hence, the idea is to sample from a conditional distribution constructed by considering one symbol at a time and conditioning on the rest of the $MN-1$ symbols. The core idea of detection using GS is to iteratively sample from the symbol-wise conditional pdf while assuming that the rest of the $MN-1$ symbols are fixed. It is established that after sufficient iterations, the samples drawn from the conditional distributions approach to those drawn from the joint distribution in (18), thereby providing the optimal solution [12]. The GS algorithm is described below.

An initial vector $\mathbf{x}^0 \in \mathbb{C}^{MN\times 1}$ drawn from $\mathbb{A}$ is considered at the start of the algorithm. We consider initialization with random vector. In the $(j+1)$th iteration, the MN symbols are updated by sampling from the following distributions:

$$\begin{aligned}
x_1^{j+1} &\sim \text{P}(x_1|x_2^j, x_3^j, \cdots, x_{MN}^j, \mathbf{y}, \mathbf{H}) \\
x_2^{j+1} &\sim \text{P}(x_2|x_1^{j+1}, x_3^j, \cdots, x_{MN}^j, \mathbf{y}, \mathbf{H}) \\
x_3^{j+1} &\sim \text{P}(x_3|x_1^{j+1}, x_2^{j+1}, \cdots, x_{MN}^j, \mathbf{y}, \mathbf{H}) \\
&\vdots \\
x_{MN}^{j+1} &\sim \text{P}(x_{MN}|x_1^{j+1}, x_2^{j+1}, \cdots, x_{MN-1}^{j+1}, \mathbf{y}, \mathbf{H}).
\end{aligned} \quad (19)$$

The conditional distribution in (19) for the kth symbol, i.e., $\text{P}(x_k = a|\mathbf{x}_{1:k-1}^{j+1}, \mathbf{x}_{k-1:MN}^j, \mathbf{y}, \mathbf{H}), a \in \mathbb{A}$ in $(j+1)$th iteration can be obtained applying Bayes rule and law of total probability to (18) as

$$\text{P}(x_k = a|\mathbf{x}_{1:k-1}^{j+1}, \mathbf{x}_{k-1:MN}^j, \mathbf{y}, \mathbf{H}) = \frac{\exp\left(\frac{||\mathbf{y}-\mathbf{H}\tilde{\mathbf{x}}||^2}{\sigma^2}\right)}{\sum_{a\in\mathbb{A}} \exp\left(\frac{||\mathbf{y}-\mathbf{H}\tilde{\mathbf{x}}||^2}{\sigma^2}\right)}, \quad (20)$$

where $\mathbf{x}_{1:k-1}^{j+1} = [x_1^{j+1} \cdots x_{k-1}^{j+1}]^T$, $\mathbf{x}_{k+1:MN}^j = [x_{k+1}^j \cdots x_{MN}^j]^T$, $\tilde{\mathbf{x}} = [x_1^{j+1} \cdots x_{k-1}^{j+1}\ a\ x_{k+1}^j \cdots x_{MN}^j]^T$, and $[\cdot]^T$ denotes transpose of a vector. After all the symbols are updated based on sampling from the corresponding conditional distribution, the ML cost is computed as

$$\phi(\mathbf{x}^{j+1}) = ||\mathbf{y} - \mathbf{H}\mathbf{x}^{j+1}||_2^2, \quad (21)$$

where $\mathbf{x}^{j+1}$ is the solution vector in $(j+1)$th iteration and $||\cdot||_2$ denotes 2-norm of a vector. The initial vector for the next iteration is updated to $\mathbf{x}^{j+1}$ if the ML cost $\phi(\mathbf{x}^{j+1}) < \phi(\mathbf{x}^j)$, else the vector $\mathbf{x}^j$ continues to be the initial vector for the subsequent iteration. The iterations continue until $j = J_{\max}$, where $J_{\max}$ is the maximum number of iterations after which the algorithm stops. Amongst the resultant $J_{\max}$ vectors, the one with minimum ML cost is returned as the detected vector. Note that, theoretically it has been proven that asymptotically

A probability mass function (pmf) over the constellation symbols in $\mathbb{A}$ is constructed for each symbol $x_k, k = 1,2,\cdots,MN$, and that constellation symbol with maximum probability is assigned to x_k.

the distribution approaches to the joint distribution in (18) thereby ensuring the convergence to the optimal solution. However, in practice, the Markov chain is observed to take prohibitively long time before it reaches the stationary distribution. One reason for this issue is stalling. It is a condition where the algorithm gets into a local trap, i.e., it gets stuck in a particular state for which the transition probability to any other state is close to zero. Hence, the Markov chain takes a long time before it eventually comes out of that state. It is observed that this results in BER degradation at high signal-to-noise ratios (SNR) [10], [11].

The problem of stalling in GS can be circumvented by sampling from a mixed distribution instead of sampling purely from the true target distribution [11]. This is the basic idea in MGS. Sampling from a weighted sum of uniform distribution $U[0,1]$ and the target joint distribution in (18) allows the Markov chain to escape the local trap and converge quickly in finite number of iterations. In addition, using a tilted distribution of the target distribution with a temperature parameter α in place of the target distribution can offer better convergence characteristics and performance. The modified target distribution with temperature parameter α is given by

$$\mathrm{P}(\mathbf{x}|\mathbf{y},\mathbf{H}) \propto \exp\left(\frac{||\mathbf{y}-\mathbf{H}\mathbf{x}||^2}{\alpha^2\sigma^2}\right), \tag{22}$$

where α is a tunable positive parameter that controls the mixing time of the Markov chain. A higher value of α implies a faster mixing of the Markov chain and hence convergence to stationary distribution in less number of iterations. The resulting mixture distribution proposed in this work is

$$\mathrm{P}(\mathbf{x}|\mathbf{y},\mathbf{H}) \propto (1-q)\psi(\alpha_1) + q\psi(\alpha_2), \tag{23}$$

where $\psi(\alpha_1) \propto \exp\left(\frac{||\mathbf{y}-\mathbf{H}\mathbf{x}||^2}{\alpha_1^2\sigma^2}\right)$ with $\alpha_1 > 1$ and $\psi(\alpha_2) \sim U[0,1]$, i.e., $\alpha_2 = \infty$. The optimum value of q that minimizes the expected number of iterations required to reach the global minima solution for first time has been observed to be the inverse of number of dimensions in the transmit vector [11]. Hence, $q = 1/MN$ is used. The MGS algorithm is listed in **Algorithm 1**. The per-symbol complexity is quadratic in MN, i.e., $\mathcal{O}(M^2N^2)$. In Sec. IV, we will compare the performance of the above MGS detector with the performance of MMSE and MP detectors, which are briefly described below.

Algorithm 1 MGS algorithm

Inputs: $\mathbf{y}, \mathbf{H}$, maximum # iterations $J_{\max}$
Initialize: $\mathbf{z} = \mathbf{x}^0$, iteration index $j = 1$, $q = \frac{1}{MN}$, $c(1) = \phi(\mathbf{x}^0)$
while $j < J_{\max}$ **do**
  for $k = 1 : MN$ **do**
    generate $\lambda \sim U[0,1]$
    if $\lambda > q$
      $x_k^{j+1} \sim \mathrm{P}(x_k|x_1^{j+1}, \cdots, x_{k-1}^{j+1}, x_k^j, x_{MN}^j, \mathbf{y}, \mathbf{H})$
    else
      $x_k^{j+1} \sim U[0,1]$
    end if
  end for
  update $c(j+1) = \phi(\mathbf{x}^{j+1})$
  if $c(j+1) < c(j)$
    $\mathbf{z} = \mathbf{x}^{j+1}$
  else
    $\mathbf{z} = \mathbf{x}^j$
  end if
  update $j = j + 1$
until $j = J_{\max}$
Obtain $m = \underset{j=1\cdots J_{\max}}{\arg\min}\, c(j)$
Output: $\hat{\mathbf{x}}_{\text{MGS}} = \mathbf{x}^m$

B. LMMSE detector

Linear MMSE (LMMSE) detector performs Euclidean distance based symbol-by-symbol detection after performing the linear equalization of the channel. For the system model in (15), the linear equalizer $\mathbf{H}_{\text{MMSE}}$ is obtained by minimizing the mean squared error between the transmit vector and the linearly equalized received vector as

$$\mathbf{H}_{\text{MMSE}} = \underset{\mathbf{A}}{\arg\min}\, \mathbb{E}\left[||\mathbf{x} - \mathbf{A}\mathbf{y}||_2^2\right]. \tag{24}$$

$\mathbf{H}_{\text{MMSE}} = (\mathbf{H}^H\mathbf{H} + \sigma^2\mathbf{I}_{MN})^{-1}\mathbf{H}^H$ is obtained upon solving the optimization problem in (24). The computation of the $\mathbf{H}_{\text{MMSE}}$ involves computing the inverse of an $MN \times MN$ matrix, which incurs a complexity of $\mathcal{O}(M^3N^3)$, and a per-symbol detection complexity of $\mathcal{O}(M^2N^2)$.

C. Message passing detector [13], [14]

The MP detector is an iterative symbol-by-symbol MAP detection algorithm that works on the principle of belief propagation. The algorithm solves the optimization problem

$$\hat{x}_j = \underset{x_j \in \mathbb{A}}{\arg\max}\, \mathrm{P}(x_j|\mathbf{y},\mathbf{H}), \tag{25}$$

by constructing a factor graph with received symbols as observation nodes and transmit symbols as variable nodes. The resultant factor graph is fully connected, i.e, it has loops and therefore results in an approximate solution. In each iteration, likelihood vectors and a posterior probability vectors are exchanged on the edges between the observation and variable nodes as messages. A Gaussian approximation of interference is adopted in the construction of the messages, which reduces complexity. The algorithm returns the pmf for each symbol once the stopping criteria is met. The symbol-wise detection complexity for MP detection is $\mathcal{O}(M^2N^2)$.

IV. Results and discussions

In this section, we present the BER performance of Zak-OTFS using the detectors discussed in Sec. III. For all the results in this section, a doubly-spread channel with P resolvable paths and uniform power delay profile is considered. The path delays are assumed to be uniformly distributed as $\tau_i \sim U[0, \tau_{\max}]$ and path Dopplers are generated using the

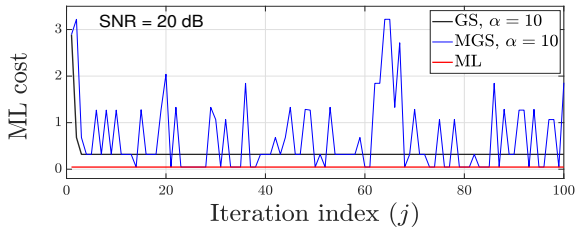

(a) ML cost evolution

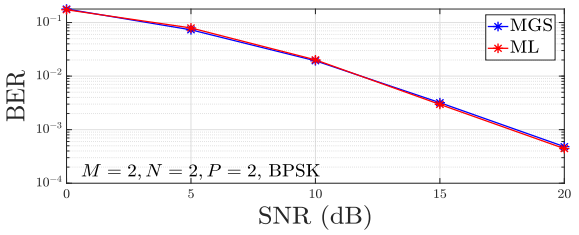

(b) BER vs SNR

Fig. 2: Performance comparison between MGS vs ML detectors for $M = 2, N = 2$, and BPSK. MGS achieves almost ML performance.

Jake's formula $\nu_i = \nu_{\max} cos(\theta)$, where $\theta \sim U[0, 2\pi]$, and $\tau_{\max}$ and $\nu_{\max}$ are the maximum delay and Doppler spreads of the channel, respectively. Channel is assumed to be perfectly known at the receiver. The DD domain transmit and receive filters are considered to be sinc filters given by

$$w_{\text{tx}}(\tau, \nu) = w_{\text{rx}}(\tau, \nu) = \sqrt{BT} sinc(B\tau) sinc(T\nu). \quad (26)$$

In conventional Gibbs sampling (GS) and mixed Gibbs sampling (MGS) detectors, we consider a random initial vector and $J_{\max} \approx 20MN$.

A. BER vs SNR comparison between MGS and ML detection

To compare the performance of the proposed MGS algorithm with that of ML, we consider a Zak-OTFS system with a small frame size, where $B = 7.5$ kHz, $T = 0.523$ ms, $P = 2$. The information symbols are drawn from BPSK constellation. The Doppler and delay periods are $\nu_p = 3.75$ kHz and $\tau_p = 1/\nu_p = 0.2667$ ms, respectively. Hence, $M = \frac{B}{\nu_p} = 2$ and $N = \frac{T}{\tau_p} = 2$. The path delays and Dopplers are $[\tau_1, \tau_2] = [0, 0.133]$ ms and $[\nu_1, \nu_2] = [0, 0]$ kHz, respectively. Figure 2(a) shows the evolution of the ML cost $\|\mathbf{y} - \mathbf{H}\mathbf{x}^j\|^2$ of the GS and MGS algorithms over iterations at an SNR of 20 dB. The cost obtained using ML detection is also plotted for reference. It is observed that the cost achieved by GS algorithm floors as the iterations progress indicating a local trap. However, the MGS algorithm is able to escape the local traps (indicated by fluctuations in the cost) and achieve the true ML cost multiple times over the iterations. This translates into a BER performance which is almost same as that of the ML detector, as can be observed in Fig. 2(b).

We next consider a Zak-OTFS system with a larger frame size where the bandwidth $B = 180$ kHz and frame duration $T = 0.467$ ms. The Doppler period is $\nu_p = 15$ kHz. Hence, $M = 12$ and $N = 7$. The information symbols are drawn from

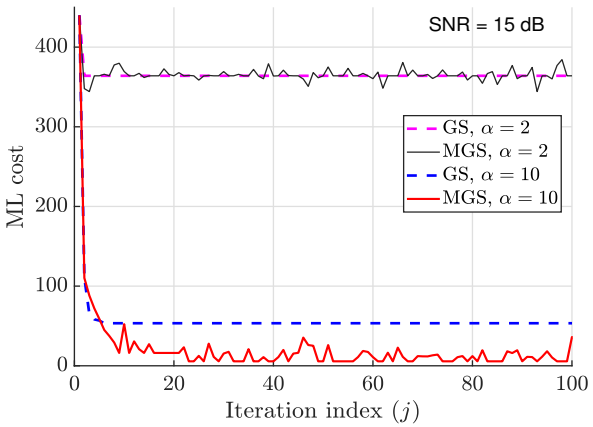

Fig. 3: Evolution of the ML cost of the state vector as a function of iteration index for $M = 12, N = 7$, and 4-QAM.

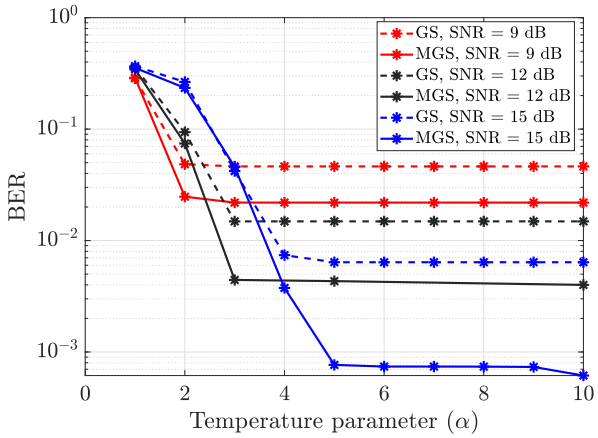

Fig. 4: BER as a function of the temperature parameter α in the MGS algorithm for $M = 12, N = 7$, and 4-QAM.

4-QAM constellation. The channel is considered to have $P = 4$ paths with $\tau_{\max} = 22.23$ μs and $\nu_{\max} = 6.424$ kHz (chosen parameters ensure the operation in the crystalline regime, i.e., $\tau_{\max} < \tau_p$ and $\nu_{\max} < \nu_p$ [5]).

B. Convergence behaviour of GS and MGS algorithms

Figure 3 captures the progression of the GS and MGS algorithms over iterations. The progression is shown in terms of the ML cost of the state vector at each iteration. The convergence trend of the GS and MGS algorithms for $\alpha = 2, 10$ is captured at an SNR of 15 dB. It is observed that the ML cost falls drastically with iterations till $j \approx 10$. Beyond this, it is observed that the GS algorithm cost remains constant indicating a local trap, while the MGS algorithm escapes the trap multiple times. For $\alpha = 2$, the ML cost achieved by both the algorithms is quite high. With $\alpha = 10$ both the algorithms achieve a low ML cost, with cost of MGS being consistently below that obtained using GS.

C. Effect of temperature parameter.

Figure 4 shows the BER performance of GS and MGS algorithms as a function of α for three SNR values, viz. 9

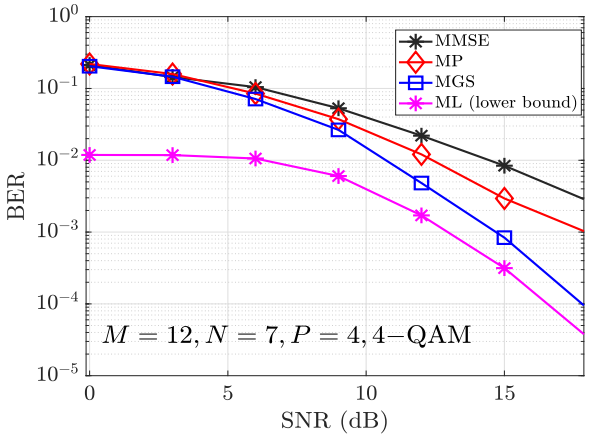

Fig. 5: BER vs SNR performance of Zak-OTFS using MMSE, MP, and MGS detectors. ML lower bound is also shown.

dB, 12 dB, and 15 dB. The performance of both GS and MGS algorithms saturate, i.e., remains almost constant after a certain α. The results show an early onset of saturation at low SNRs, i.e, for SNR of 9 dB, the performance flattens at $\alpha = 2$, while the saturation occurs at $\alpha = 3$ and 5 for SNR of 12 and 15 dB, respectively. The performance of the MGS algorithm is significantly superior compared to that obtained using GS algorithm for all the three SNRs. Further, post saturation, the gap between the performance of GS and MGS algorithms is seen to progressively increase as SNR increases. Since the choice of α does not add to the complexity, we fix $\alpha = 10$ for the subsequent simulations.

D. Comparison of BER vs SNR for different detectors

Figure 5 shows the BER vs SNR performance comparison between the MMSE, MP, and MGS detectors described in Sec. III. In order to compare the MGS performance with ML performance for the large frame size considered, we obtained a lower bound on ML performance using the reactive tabu search (RTS) algorithm in [15] with one-symbol neighborhood. This ML lower bound is also plotted in Fig. 5 for comparison. It is observed that the performance of MMSE detector is sub-par. The MP algorithm performance is superior to MMSE performance but is still far from the ML lower bound. Whereas, the MGS algorithm performance is superior to both MMSE and MP detectors performance. In addition, the MGS performance is found to be quite close to the ML lower bound, and this illustrates the effectiveness of the proposed MGS approach for Zak-OTFS detection.

V. Conclusion

We presented an early investigation of near-optimal detection of Zak-OTFS signals. Exhaustive enumeration based optimum ML and MAP detection become prohibitive in complexity as the OTFS frame size grows. MMSE detector was employed in the early papers on Zak-OTFS. However, the performance of MMSE detector is far from optimum. MP detection can provide superior performance compared to MMSE performance, but is inferior in comparison with the optimum ML performance. We proposed a mixed Gibbs sampling based detection algorithm which performed close to the optimum ML performance at low detection complexity. Sampling from a mixed distribution (weighted sum of uniform and target distributions) aided the algorithm to quickly exit from stalling and achieve near-optimal performance at low complexity. A lower bound on the ML performance obtained using reactive tabu search with one-symbol neighborhood was used to establish the closeness of the proposed MGS performance to the optimum ML performance. Investigation of several other algorithms for efficient signal detection and channel estimation for Zak-OTFS remains open, which can be explored as future work.

References

[1] R. Hadani et al., "Orthogonal time frequency space modulation," *Proc. IEEE WCNC'2017*, pp. 1-6, Mar. 2017

[2] Y. Hong, T. Thaj, and E. Viterbo, *Delay-Doppler Communications: Principles and Applications*, Academic Press, 2022.

[3] "Best Readings in Orthogonal Time Frequency Space (OTFS) and Delay Doppler Signal Processing," June 2022. https://www.comsoc.org/publications/best-readings/orthogonal-time-frequency-space-otfs-and-delay-doppler-signal-processing

[4] A. J. E. M. Janssen, "The Zak transform: a signal transform for sampled time-continuous signals," *Philips J. Res.*, 43, pp. 23-69, 1988.

[5] S. K. Mohammed, R. Hadani, A. Chockalingam, and R. Calderbank, "OTFS - a mathematical foundation for communication and radar sensing in the delay-Doppler domain," *IEEE BITS the Information Theory Magazine*, vol. 2, no. 2, pp. 36-55, Nov. 2022.

[6] S. K. Mohammed, R. Hadani, A. Chockalingam, and R. Calderbank, "OTFS - predictability in the delay-Doppler domain and its value to communication and radar sensing," *IEEE BITS the Information Theory Magazine*, IEEE early access, doi: 10.1109/MBITS.2023.3319595.

[7] D. J. C. MacKay, *Information Theory, Inference and Learning Algorithms*, Cambridge Univ. Press, 2003.

[8] E. Panayirci, H. Dogan and H. V. Poor, "A Gibbs sampling based MAP detection algorithm for OFDM over rapidly varying mobile radio channels," *Proc. IEEE GLOBECOM'2009*, pp. 1-6, Nov. 2009.

[9] M. Hansen, B. Hassibi, A. G. Dimakis and W. Xu, "Near-optimal detection in MIMO systems using Gibbs sampling," *Proc. IEEE GLOBECOM'2009*, pp. 1-6, Nov. 2009.

[10] R. Peng, R-R. Chen, and B. Farhang-Boroujeny, "Markov chain Monte Carlo detectors for channels with intersymbol interference," *IEEE Trans. Signal Process.*, vol. 58, no. 4, pp. 2206-2217, Apr. 2010.

[11] T. Datta, N. A. Kumar, A. Chockalingam, and B. S. Rajan, "A novel Monte-Carlo-sampling-based receiver for large-scale uplink multiuser MIMO systems," *IEEE Trans. Veh. Tech.,*, vol. 62, no. 7, pp. 3019-3038, Sep. 2013.

[12] Rong Chen, J. S. Liu and Xiaodong Wang, "Convergence analyses and comparisons of Markov chain Monte Carlo algorithms in digital communications," IEEE Trans. Sig. Proc., vol. 50, no. 2, pp. 255-270, Feb. 2002.

[13] P. Som, T. Datta, N. Srinidhi, A. Chockalingam and B. S. Rajan,"Low-complexity detection in large-dimension MIMO-ISI channels using graphical models", *IEEE J. Sel. Topics Sig. Proc.*, vol. 5, no. 8, pp. 1497-1511, Dec. 2011.

[14] P. Raviteja, K. T. Phan, Y. Hong, and E. Viterbo, "Interference cancellation and iterative detection for orthogonal time frequency space modulation," *IEEE Trans. Wireless Commun.,* vol. 17, no. 10, pp. 6501-6515, Aug. 2018.

[15] N. Srinidhi, T. Datta, A. Chockalingam and B. S. Rajan, "Layered tabu search algorithm for large-MIMO detection and a lower bound on ML performance," *IEEE Trans. Commun.*, vol. 59, no. 11, pp. 2955-2963, Nov. 2011.